Journal of
Mechanics of
Materials and Structures

ANALYTICAL SOLUTION FOR A CONCENTRATED FORCE
ON THE FREE SURFACE OF A COATED MATERIAL

Zhigen Wu, Yihua Liu, Chunxiao Zhan and Meiqin Wang

ANALYTICAL SOLUTION FOR A CONCENTRATED FORCE ON THE FREE SURFACE OF A COATED MATERIAL

ZHIGEN WU, YIHUA LIU, CHUNXIAO ZHAN AND MEIQIN WANG

Based on the general solution of the displacement method for isotropic plane problems, the analytical solution for the plane problem of coated materials subjected to an arbitrary concentrated force on the free surface has been derived explicitly by using the image point method. The displacement functions are assumed to be the infinite series of the harmonic functions defined in the local coordinate systems with their origins placed at different image points. The harmonic functions corresponding to the higher-order image points can be deduced from those to the lower-order points by the recurrence formulae presented in this paper, and the first two harmonic functions are the displacement functions for the solution of a semi-infinite plane subjected to a concentrated force on the free surface. The theoretical formulae have been confirmed by numerical, finite-element-based, results in a special coated material.

1. Introduction

With the wide application of film-coated and surface-treated materials in engineering structures, the stress and failure analysis of coated materials have been the focus of attention. To obtain interfacial stresses for the evaluation of the cohesive strength, there are commonly three approaches: analytical, numerical, and experimental. In the last two decades, some numerical studies [Djabella and Arnell 1993; Hiroyuki et al. 1994b; Hiroyuki et al. 1994a; Kouitat-Njiwa and von Stebut 2003] and experimental methods [Masayuki et al. 1994; Takuma et al. 2000] have been developed. However, accurate stress results at the interface cannot be obtained easily by numerical or experimental methods for reasons of the thin coating or surface layer. Therefore, an analytical solution for coated materials is desirable.

For coated materials with a thin surface layer, the analytical solution of the stress field cannot be deduced easily by the theoretical method due to the difficulty in satisfying boundary and interface conditions. In recent years, the image point method has been applied to the construction of stress or displacement functions and the analytical solutions of coated materials for some cases have been obtained. The image point method is a technique that uses the superposition of known solutions to construct the solution of other complicated problems, and the relevant stress or displacement functions are expressed in the form corresponding to the loading point or image points. To our knowledge, this method was first employed by Mindlin [1936], who dealt with the fundamental solution for a single force applied in the interior of a semi-infinite solid, and the solution may be called a half-space nucleus of strain. Subsequently, Mindlin and Cheng [1950] provided many fundamental solutions for nuclei of strain in the half-space solid. Rongved [1955] found the theoretical solution of a point force acting in the interior of one of the two jointed half-spaces. Dundurs and Hetényi [1965] presented the fundamental solution for a point

force applied in the interior of one of the two elastic half-spaces jointed by a sliding contact interface. Phan-Thien [1983] considered the case of an elastic half-space with a fixed boundary. Hasegawa *et al.* [1992] investigated Green's function for the axisymmetric problem of a bimaterial elastic solid. Recently, Ma and Lin [2001; 2002b] researched Green's functions for an isotropic elastic half-plane and bimaterial subjected to forces and dislocations, and nearly all kinds of image singularities for both half-plane and bimaterial were discussed in considerable detail. In these studies, one reflection face exists and the image point is a single point as far from the face as the object point. If there are two parallel reflection faces, the object point will lead to infinite image points by reciprocal reflections. Therefore, the image point method can be also extended to solve the problem with two parallel faces, and the related stress or displacement functions are constructed in the form of infinite series about the image points. For example, by taking the two interfaces as reflection faces, Aderogba [2003] established a theorem to generate the Airy stress function for trimaterials comprised of two semi-infinite planes separated by a thick layer due to a point force applied in or near the intermediate layer. By adopting the interface and surface as the reflection faces, Xu and Mutoh [2003a; 2003b] derived the analytical solutions for both two- and three-dimensional problems of coated semi-infinite bodies subjected to a concentrated force on the surface. By introducing two series image points, Li and Xu [2004; 2007] obtained the fundamental solutions for a coated semi-infinite plane subjected to a concentrated force in the interior of the coating layer and substrate as well as at the interface. Most recently, Yang and Xu [2009] deduced the three-dimensional analytical solution of coated materials with concentrated forces in the interior of the coating layer.

In the literature above, the image method was applied to isotropic materials. In fact, this method can also be applied to anisotropic materials. For example, Willis [1970] and Barnett and Lothe [1974] considered Green's functions for the two-dimensional deformation of an anisotropic elastic half-space subjected to a line force and/or a line dislocation inside it. Ting [1992] discussed in detail the image singularities of Green's functions for an anisotropic elastic half-space and bimaterials subjected to line forces and line dislocations based on Stroh's formalism. It should be mentioned that the locations of image singularities of Green's functions for the half-plane depend on anisotropic elastic constants and there are at most nine image points located at different positions with respect to the object point. Therefore, it is difficult to apply the conventional image method to obtain the solution of the anisotropic problem with two reflection faces directly. Nevertheless, recently, some particular mathematical approaches were employed by fewer researchers to treat certain layered half-planes with complex material constants. For instance, by using the Lekhnitskii formalism for anisotropic elastic materials and the Fourier-transformation technique, Ma and Lin [2002a] obtained the analytical solutions for stresses in the anisotropic layered half-plane subjected to concentrated forces and edge dislocations in the thin layer or in the half-plane. Applying the Fourier transform method and the series expansion technique, an effective analytic methodology was developed by Ma and Lee [2009] to construct the full-field explicit solutions for a transversely isotropic magnetoelectroelastic layered half-plane subjected to generalized line forces and edge locations. In these problems, the complete solutions consist of the simplest solutions for the infinite medium with applied loadings, and the physical meaning of these simplest solutions is the image method.

In this paper, in order to obtain the explicit analytical solution for coated materials subjected to an arbitrary concentrated force on the free surface, we make use of the general solution of the displacement method as well as the image point method to construct the displacement functions in terms of infinite series of harmonic functions. According to the free boundary and interface continuity conditions, the
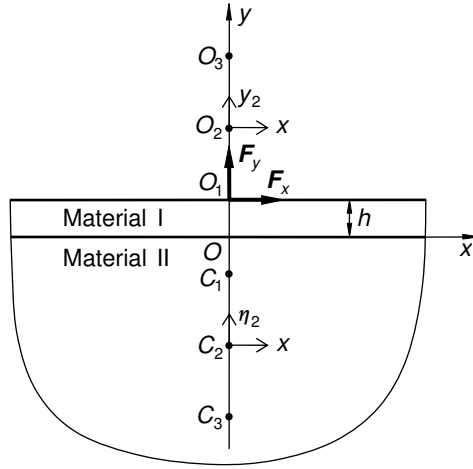
Figure 1. Analytical model of a coated material.

recurrence formulae for the harmonic functions are derived and all harmonic functions can be determined from the initial harmonic functions, which correspond to the first-order image point and are the displacement functions for the semi-infinite plane subjected to a concentrated force on the free surface.

2. Analytical model

The coated material is modeled as a surface layer with thickness h bonded perfectly to a half-plane, as shown in Figure 1. An arbitrary concentrated force is decomposed into a normal force F_x and a tangential force F_y applied at the point O_1 on the free surface of the surface layer. The surface layer and half-plane materials are numbered I and II, respectively; their shear moduli and Poisson's ratios are μ_I, μ_{II}, ν_I, and ν_{II}. We place the origin O of the global coordinate system on the interface just beneath the loading point O_1 and the x-axis along the interface. By use of the reciprocal reflections of the loading point O_1 on the interface and free surface, infinite image points will be produced on the xy-plane, i.e., the image points O_k $(k = 1, 2, 3, \ldots)$ in the upper half-plane and C_k $(k = 1, 2, 3, \ldots)$ in the lower half-plane. Introducing the local coordinates (x, y_k) and (x, η_k) with their origins located at O_k and C_k, respectively, the relationships between the local and global coordinates can be expressed as

$$y_k = y - (2k - 1)h, \quad \eta_k = y + (2k - 1)h, \quad k = 1, 2, 3, \ldots. \tag{1}$$

The displacement and traction continuity conditions on the interface can be represented as

$$u_I = u_{II}, \quad v_I = v_{II}, \quad \sigma_{yI} = \sigma_{yII}, \quad \tau_{xyI} = \tau_{xyII}, \quad \text{at } y = 0, \tag{2}$$

and the free surface condition can be written as

$$\sigma_{yI} = 0, \quad \tau_{xyI} = 0, \quad \text{at } y = h, \tag{3}$$

where subscript I and II refer to materials I and II, respectively.

3. Derivation of theoretical formulae

The general solution of the displacement method for isotropic plane problems can be obtained from [Wu and Liu 2008] as

$$2\mu u = \frac{\partial \Phi}{\partial x} + y \frac{\partial \Psi}{\partial x}, \quad 2\mu v = \frac{\partial \Phi}{\partial y} + y \frac{\partial \Psi}{\partial y} - \kappa \Psi, \tag{4}$$

$$\sigma_x = \frac{\partial^2 \Phi}{\partial x^2} + y \frac{\partial^2 \Psi}{\partial x^2} + \frac{\kappa - 3}{2} \frac{\partial \Psi}{\partial y}, \quad \sigma_y = \frac{\partial^2 \Phi}{\partial y^2} + y \frac{\partial^2 \Psi}{\partial y^2} - \frac{\kappa + 1}{2} \frac{\partial \Psi}{\partial y},$$

$$\tau_{xy} = \frac{\partial^2 \Phi}{\partial x \partial y} + y \frac{\partial^2 \Psi}{\partial x \partial y} - \frac{\kappa - 1}{2} \frac{\partial \Psi}{\partial x}, \tag{5}$$

where Φ and Ψ are the two displacement functions which are harmonic, μ is the shear modulus, $\kappa = 3 - 4\nu$ for plane strain and $(3 - \nu)/(1 + \nu)$ for plane stress, and ν is Poisson's ratio.

Substituting (4) and (5) into (2) and (3), respectively, one has

$$\Gamma \Phi_{\mathrm{I}} = \Phi_{\mathrm{II}}, \quad \Gamma \left(\frac{\partial \Phi_{\mathrm{I}}}{\partial y} - \kappa_{\mathrm{I}} \Psi_{\mathrm{I}} \right) = \frac{\partial \Phi_{\mathrm{II}}}{\partial y} - \kappa_{\mathrm{II}} \Psi_{\mathrm{II}},$$

$$\frac{\partial^2 \Phi_{\mathrm{I}}}{\partial y^2} - \frac{\kappa_{\mathrm{I}} + 1}{2} \frac{\partial \Psi_{\mathrm{I}}}{\partial y} = \frac{\partial^2 \Phi_{\mathrm{II}}}{\partial y^2} - \frac{\kappa_{\mathrm{II}} + 1}{2} \frac{\partial \Psi_{\mathrm{II}}}{\partial y}, \quad \frac{\partial \Phi_{\mathrm{I}}}{\partial y} - \frac{\kappa_{\mathrm{I}} - 1}{2} \Psi_{\mathrm{I}} = \frac{\partial \Phi_{\mathrm{II}}}{\partial y} - \frac{\kappa_{\mathrm{II}} - 1}{2} \Psi_{\mathrm{II}}, \quad \text{at } y = 0, \tag{6}$$

where $\Gamma = \mu_{\mathrm{II}}/\mu_{\mathrm{I}}$, and

$$\frac{\partial^2 \Phi_{\mathrm{I}}}{\partial y^2} + h \frac{\partial^2 \Psi_{\mathrm{I}}}{\partial y^2} - \frac{\kappa_{\mathrm{I}} + 1}{2} \frac{\partial \Psi_{\mathrm{I}}}{\partial y} = 0, \quad \frac{\partial \Phi_{\mathrm{I}}}{\partial y} + h \frac{\partial \Psi_{\mathrm{I}}}{\partial y} - \frac{\kappa_{\mathrm{I}} - 1}{2} \Psi_{\mathrm{I}} = 0, \quad \text{at } y = h. \tag{7}$$

In order to solve the displacement functions Φ_{I}, Ψ_{I}, Φ_{II}, and Ψ_{II}, assume that these functions can be written in series form as

$$\Phi_{\mathrm{I}} = \sum_{k=1}^{\infty} [A_k(x, y_k) + \phi_k(x, \eta_k)], \quad \Phi_{\mathrm{II}} = \sum_{k=1}^{\infty} B_k(x, y_k),$$

$$\Psi_{\mathrm{I}} = \sum_{k=1}^{\infty} [a_k(x, y_k) + \psi_k(x, \eta_k)], \quad \Psi_{\mathrm{II}} = \sum_{k=1}^{\infty} b_k(x, y_k), \tag{8}$$

where A_k, ϕ_k, a_k, ψ_k, B_k, and b_k are harmonic functions with respect to x and y_k or η_k. Considering the remote stress condition (the stresses should vanish at infinite), all functions on the right in (8) must be singular at their corresponding origins. Since there is no stress singularity in the material II, the displacement functions of the material II cannot contain any term related to the image points in the lower half-plane.

From (1), it is easy to find that

$$\frac{\partial}{\partial y} = \frac{\partial}{\partial y_k}, \quad \frac{\partial}{\partial y} = \frac{\partial}{\partial \eta_k}. \tag{9}$$

Substituting (8) into (6) and using (9), one obtains, at $y = 0$,

$$\Gamma\phi_k(x, \eta_k) = B_k(x, y_k) - \Gamma A_k(x, y_k),$$

$$\Gamma\left[\frac{\partial\phi_k(x, \eta_k)}{\partial\eta_k} - \kappa_\mathrm{I}\psi_k(x, \eta_k)\right] = \frac{\partial B_k(x, y_k)}{\partial y_k} - \kappa_\mathrm{II}b_k(x, y_k) - \Gamma\left[\frac{\partial A_k(x, y_k)}{\partial y_k} - \kappa_\mathrm{I}a_k(x, y_k)\right],$$

$$\frac{\partial^2\phi_k(x, \eta_k)}{\partial\eta_k^2} - \frac{\kappa_\mathrm{I}+1}{2}\frac{\partial\psi_k(x, \eta_k)}{\partial\eta_k} = \frac{\partial^2 B_k(x, y_k)}{\partial y_k^2} - \frac{\kappa_\mathrm{II}+1}{2}\frac{\partial b_k(x, y_k)}{\partial y_k} - \frac{\partial^2 A_k(x, y_k)}{\partial y_k^2} + \frac{\kappa_\mathrm{I}+1}{2}\frac{\partial a_k(x, y_k)}{\partial y_k},$$

$$\frac{\partial\phi_k(x, \eta_k)}{\partial\eta_k} - \frac{\kappa_\mathrm{I}-1}{2}\psi_k(x, \eta_k) = \frac{\partial B_k(x, y_k)}{\partial y_k} - \frac{\kappa_\mathrm{II}-1}{2}b_k(x, y_k) - \frac{\partial A_k(x, y_k)}{\partial y_k} + \frac{\kappa_\mathrm{I}-1}{2}a_k(x, y_k). \quad (10)$$

These equations are of the form $L(x, \eta_k) = R(x, y_k)$ (L and R being the left and right sides of the equation, respectively). Because (10) is valid only on the interface where the local coordinate values satisfy $y_k = -\eta_k = -(2k - 1)h$, we have the interchange laws

$$\frac{\partial L}{\partial\eta_k} = -\frac{\partial R}{\partial y_k}, \quad \int L\,\mathrm{d}\eta_k = -\int R\,\mathrm{d}y_k. \quad (11)$$

Applying (11) to (10), we obtain

$$B_k(x, y_k) = \frac{\Gamma(\kappa_\mathrm{I}+1)}{\Gamma\kappa_\mathrm{I}+1}A_k(x, y_k) + \Gamma\left[\frac{\kappa_\mathrm{I}^2(\Gamma - 1)}{2(\Gamma\kappa_\mathrm{I}+1)} - \frac{\Gamma\kappa_\mathrm{I} - \kappa_\mathrm{II}}{2(\Gamma + \kappa_\mathrm{II})}\right]\int a_k(x, y_k)\,\mathrm{d}y_k,$$

$$b_k(x, y_k) = \frac{\Gamma(\kappa_\mathrm{I}+1)}{\Gamma + \kappa_\mathrm{II}}a_k(x, y_k), \quad (12)$$

$$\phi_k(x, \eta_k) = -\frac{\kappa_\mathrm{I}(\Gamma - 1)}{\Gamma\kappa_\mathrm{I}+1}A_k(x, y_k) + \left[\frac{\kappa_\mathrm{I}^2(\Gamma - 1)}{2(\Gamma\kappa_\mathrm{I}+1)} - \frac{\Gamma\kappa_\mathrm{I} - \kappa_\mathrm{II}}{2(\Gamma + \kappa_\mathrm{II})}\right]\int a_k(x, y_k)\,\mathrm{d}y_k,$$

$$\psi_k(x, \eta_k) = \frac{2(\Gamma - 1)}{\Gamma\kappa_\mathrm{I}+1}\frac{\partial A_k(x, y_k)}{\partial y_k} - \frac{\kappa_\mathrm{I}(\Gamma - 1)}{\Gamma\kappa_\mathrm{I}+1}a_k(x, y_k), \quad \text{at } y_k = -\eta_k. \quad (13)$$

Equations (12) and (13) show that the four harmonic functions B_k, b_k, ϕ_k, and ψ_k can be calculated by using the other two ones, A_k and a_k. In (13), $y_k = -\eta_k$ means that y_k on the right side should be replaced by $-\eta_k$ to obtain ϕ_k and ψ_k.

Substituting the values of Φ_I and Ψ_I from (8) into (7), using the relation (9), and considering the symmetric relations of the image points O_{k+1} and C_k about the free surface, we have

$$\frac{\partial^2 A_{k+1}(x, y_{k+1})}{\partial y_{k+1}^2} + h\frac{\partial^2 a_{k+1}(x, y_{k+1})}{\partial y_{k+1}^2} - \frac{\kappa_\mathrm{I}+1}{2}\frac{\partial a_{k+1}(x, y_{k+1})}{\partial y_{k+1}}$$

$$= -\left[\frac{\partial^2\phi_k(x, \eta_k)}{\partial\eta_k^2} + h\frac{\partial^2\psi_k(x, \eta_k)}{\partial\eta_k^2} - \frac{\kappa_\mathrm{I}+1}{2}\frac{\partial\psi_k(x, \eta_k)}{\partial\eta_k}\right],$$

$$\frac{\partial A_{k+1}(x, y_{k+1})}{\partial y_{k+1}} + h\frac{\partial a_{k+1}(x, y_{k+1})}{\partial y_{k+1}} - \frac{\kappa_\mathrm{I}-1}{2}a_{k+1}(x, y_{k+1})$$

$$= -\left[\frac{\partial\phi_k(x, \eta_k)}{\partial\eta_k} + h\frac{\partial\psi_k(x, \eta_k)}{\partial\eta_k} - \frac{\kappa_\mathrm{I}-1}{2}\psi_k(x, \eta_k)\right], \quad \text{at } y = h. \quad (14)$$

and

$$\frac{\partial^2 A_1(x, y_1)}{\partial y_1^2} + h \frac{\partial^2 a_1(x, y_1)}{\partial y_1^2} - \frac{\kappa_I + 1}{2} \frac{\partial a_1(x, y_1)}{\partial y_1} = 0,$$

$$\frac{\partial A_1(x, y_1)}{\partial y_1} + h \frac{\partial a_1(x, y_1)}{\partial y_1} - \frac{\kappa_I - 1}{2} a_1(x, y_1) = 0, \quad \text{at } y = h. \tag{15}$$

Equation (14) is in the form $L(x, y_{k+1}) = R(x, \eta_k)$. On the free surface $y = h$, the local coordinate values satisfy $y_{k+1} = -\eta_k = -2kh$; thus we can get the interchange laws in the form

$$\frac{\partial L}{\partial y_{k+1}} = -\frac{\partial R}{\partial \eta_k}, \quad \int L \, dy_{k+1} = -\int R \, d\eta_k. \tag{16}$$

Applying (16) to (14), one has

$$A_{k+1}(x, y_{k+1}) = \kappa_I \phi_k(x, \eta_k) + 2h \frac{\partial \phi_k(x, \eta_k)}{\partial \eta_k} + 2h^2 \frac{\partial \psi_k(x, \eta_k)}{\partial \eta_k} - \frac{\kappa_I^2 - 1}{2} \int \psi_k(x, \eta_k) \, d\eta_k,$$

$$a_{k+1}(x, y_{k+1}) = -2 \frac{\partial \phi_k(x, \eta_k)}{\partial \eta_k} - 2h \frac{\partial \psi_k(x, \eta_k)}{\partial \eta_k} + \kappa_I \psi_k(x, \eta_k), \quad \text{at } \eta_k = -y_{k+1}. \tag{17}$$

From (17), we find that the harmonic functions A_{k+1} and a_{k+1} can be obtained from ϕ_k and ψ_k. In (17), $\eta_k = -y_{k+1}$ means that η_k on the right side should be replaced by $-y_{k+1}$ to obtain A_{k+1} and a_{k+1}. Equation (17) shows that the harmonic functions corresponding to the order $k + 1$ can be deduced from the ones to the order k. Therefore, if the functions A_1 and a_1 are given, all functions on the right in (8) can be derived by using (12), (13), and (17).

To determine the functions A_1 and a_1, one should consider simultaneously (15) and the condition of a concentrated force applied at the point O_1 on the free surface. It is not difficult to find that the solutions for the normal and tangential concentrated forces on the free surface of a semi-infinite plane satisfy these conditions. Considering the parallel translation of the coordinate system, the functions A_1 and a_1 for the normal and tangential forces can be found, respectively, as

$$A_1(x, y_1) = \frac{F_y}{2\pi} \left[\left(\frac{\kappa_I - 1}{2} y_1 - h \right) \ln(x^2 + y_1^2) + (\kappa_I - 1)x \arctan \frac{y_1}{x} \right],$$

$$a_1(x, y_1) = \frac{F_y}{2\pi} \ln(x^2 + y_1^2), \quad \text{for normal force,} \tag{18}$$

$$A_1(x, y_1) = \frac{F_x}{\pi} \left[\left(\frac{\kappa_I + 1}{2} y_1 - h \right) \arctan \frac{y_1}{x} - \frac{(\kappa_I + 1)}{4} x \ln(x^2 + y_1^2) \right],$$

$$a_1(x, y_1) = \frac{F_x}{\pi} \arctan \frac{y_1}{x}, \quad \text{for tangential force.} \tag{19}$$

It is easy to demonstrate that (18) and (19) are all harmonic functions and satisfy (15) as well as the condition of the concentrated force applied at the point O_1. To this time, all harmonic functions appearing on the right in (8) can be derived through the recurrence as shown in (12), (13), (17), and (18) or (19). Therefore, the analytical solution for coated materials subjected to an arbitrary concentrated force on the free surface is obtained explicitly.

4. Numerical results

For a verification of the correctness of the above theoretical formulae, the stresses along the interface of a coated material (Figure 2) have been numerically analyzed by ABAQUS based on the displacement finite element method concerning the plane strain analysis. Since the thickness of the surface layer is very thin, it can be considered as a thin film bonded to the free surface of a semi-infinite plane. In Figure 2, the height and width of the substrate are taken as one and two hundred times the thickness of the film, respectively. Although half of the analytical model can be selected for the numerical calculation due to the symmetry and anti-symmetry of the problem, the whole model was till treated for the numerical analysis to obtain the accurate numerical results of the nodes at and near the symmetric axis y. The finite element mesh, containing 6200 elements and 18841 nodes, is shown in Figure 3. The material constants are $E_{\mathrm{I}} = 546$ GPa, $E_{\mathrm{II}} = 206$ GPa, and $\nu_{\mathrm{I}} = \nu_{\mathrm{II}} = 0.3$, respectively.

Tables 1–4 compare the theoretical and FEM results of the stress components along the interface for the normal and tangential concentrated forces, respectively, where $n = k$ means that the orders of the image point from one to k are considered in the analytical solution. From these tables it can be observed that the higher the order of the image point is considered, the better the theoretical results agree with the FEM ones, and the convergence rates are all very rapid. From Table 1 it can be found that the maximum of the stress component σ_y is about 0.513892 MPa for the theoretical result and 0.517178 MPa for the FEM one at $x = 0$, and the relative error is 0.64%. Table 2 shows that the minimum of the stress component τ_{xy} is about -0.166807 MPa for the theoretical result and -0.168955 MPa for the FEM one at $x = 0.6$ mm, and the relative error is 1.27%. Table 3 indicates that the minimum of the stress component σ_y is about
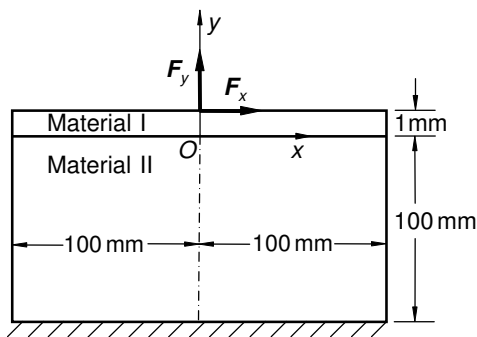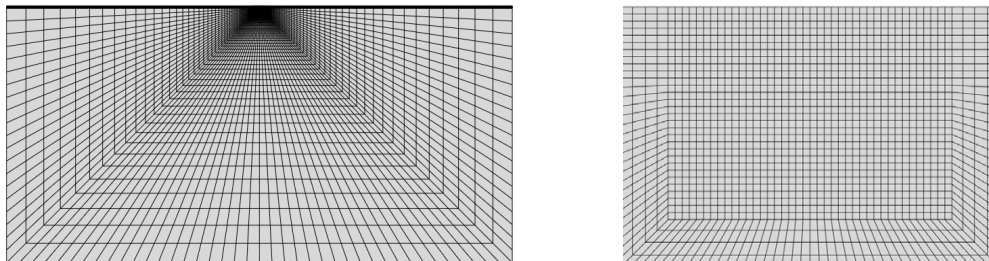

Figure 2. Model for FEM calculation.

Figure 3. Mesh division for FEM (right: zoom near the loading point).

			σ_y/MPa		
x/mm	$n=1$	$n=2$	$n=3$	$n=4$	FEM
0.0	0.377616	0.470810	0.502243	0.513892	0.517178
0.2	0.348280	0.439538	0.470597	0.482151	0.486965
0.4	0.277906	0.363634	0.393600	0.404869	0.412302
0.6	0.199702	0.277057	0.305294	0.316106	0.324809
0.8	0.134947	0.202128	0.228126	0.238330	0.246878
1.0	0.088676	0.144976	0.168376	0.177853	0.185658
1.2	0.057885	0.103544	0.124148	0.132810	0.138807
1.4	0.037974	0.073918	0.091680	0.099476	0.105742
1.6	0.025168	0.052719	0.067721	0.074633	0.080256
1.8	0.016876	0.037494	0.049923	0.055961	0.061005
2.0	0.011439	0.026542	0.036652	0.041853	0.046368
2.31919	0.006252	0.015088	0.022140	0.026092	0.029827
2.69364	0.003101	0.007558	0.011908	0.014714	0.017624
3.13291	0.001306	0.003164	0.005508	0.007284	0.009394
3.64824	0.000355	0.000952	0.002031	0.003028	0.004437
4.25279	−0.000101	0.000031	0.000472	0.000978	0.001850

Table 1. Normal stress σ_y along the interface for the case of $F_x = 0$ and $F_y = 1$ N.

			τ_{xy}/MPa		
x/mm	$n=1$	$n=2$	$n=3$	$n=4$	FEM
0.0	0.000000	0.000000	0.000000	0.000000	0.000000
0.2	−0.078466	−0.086408	−0.088172	−0.088660	−0.090259
0.4	−0.126963	−0.141976	−0.145389	−0.146345	−0.148621
0.6	−0.140036	−0.160574	−0.165427	−0.166807	−0.168955
0.8	−0.130309	−0.154459	−0.160467	−0.162210	−0.163999
1.0	−0.111587	−0.137409	−0.144241	−0.146276	−0.147799
1.2	−0.091997	−0.117795	−0.125111	−0.127359	−0.128753
1.4	−0.074835	−0.099318	−0.106796	−0.109176	−0.110524
1.6	−0.060862	−0.083188	−0.090546	−0.092981	−0.094314
1.8	−0.049829	−0.069566	−0.076578	−0.078995	−0.080316
2.0	−0.041206	−0.058242	−0.064744	−0.067084	−0.068366
2.31919	−0.031160	−0.044170	−0.049661	−0.051781	−0.052963
2.69364	−0.023304	−0.032496	−0.036728	−0.038501	−0.039528
3.13291	−0.017365	−0.023419	−0.026333	−0.027663	−0.028471
3.64824	−0.012977	−0.016778	−0.018529	−0.019392	−0.019936
4.25279	−0.009781	−0.012140	−0.013028	−0.013478	−0.013750

Table 2. Shear stress τ_{xy} along the interface for the case of $F_x = 0$ and $F_y = 1$ N.

−0.143830 MPa for the theoretical result and −0.143788 MPa for the FEM one at $x = 0.6$ mm, and the relative error is 0.03%. In Table 4, the maximum of the stress component τ_{xy} is about 0.101641 MPa for the theoretical result and 0.102782 MPa for the FEM one at $x = 1.2$ mm, and the relative error is 1.11%.

			σ_y/MPa		
x/mm	$n = 1$	$n = 2$	$n = 3$	$n = 4$	FEM
0.0	0.000000	0.000000	0.000000	0.000000	0.000000
0.2	−0.069656	−0.076721	−0.078337	−0.078804	−0.077114
0.4	−0.111162	−0.124505	−0.127639	−0.128552	−0.127132
0.6	−0.119821	−0.138045	−0.142507	−0.143830	−0.143788
0.8	−0.107958	−0.129342	−0.134879	−0.136558	−0.137641
1.0	−0.088676	−0.111488	−0.117807	−0.119778	−0.121405
1.2	−0.069462	−0.092198	−0.098999	−0.101193	−0.102991
1.4	−0.053163	−0.074696	−0.081694	−0.084038	−0.085851
1.6	−0.040268	−0.059879	−0.066827	−0.069253	−0.071031
1.8	−0.030376	−0.047714	−0.054414	−0.056860	−0.058592
2.0	−0.022878	−0.037874	−0.044183	−0.046595	−0.048302
2.31919	−0.014500	−0.026062	−0.031579	−0.033851	−0.035506
2.69364	−0.008354	−0.016731	−0.021256	−0.023285	−0.024818
3.13291	−0.004091	−0.009919	−0.013416	−0.015124	−0.016489
3.64824	−0.001295	−0.005342	−0.007950	−0.009318	−0.010482
4.25279	−0.000429	−0.002494	−0.004460	−0.005532	−0.006493

Table 3. Normal stress σ_y along the interface for the case of $F_x = 1\,\mathrm{N}$ and $F_y = 0$.

			τ_{xy}/MPa		
x/mm	$n = 1$	$n = 2$	$n = 3$	$n = 4$	FEM
0.0	−0.022910	−0.025870	−0.026507	−0.026780	−0.028217
0.2	−0.007212	−0.009495	−0.010030	−0.010127	−0.011164
0.4	0.027875	0.027507	0.027271	0.027240	0.027283
0.6	0.061111	0.063535	0.063761	0.063833	0.064659
0.8	0.081337	0.086962	0.087769	0.087976	0.089110
1.0	0.088676	0.097452	0.098904	0.099268	0.100444
1.2	0.087486	0.099000	0.101107	0.101641	0.102782
1.4	0.081859	0.095488	0.098213	0.098918	0.100030
1.6	0.074469	0.089522	0.092791	0.093660	0.094766
1.8	0.066781	0.082613	0.086326	0.087346	0.088465
2.0	0.059502	0.075575	0.079624	0.080775	0.081943
2.31919	0.049356	0.065027	0.069393	0.070705	0.071945
2.69364	0.039863	0.054403	0.058853	0.060276	0.061562
3.13291	0.031491	0.044462	0.048753	0.050214	0.051528
3.64824	0.024433	0.035721	0.039673	0.041093	0.042405
4.25279	0.018685	0.028395	0.031935	0.033254	0.034533

Table 4. Shear stress τ_{xy} along the interface for the case of $F_x = 1\,\mathrm{N}$ and $F_y = 0$.

Tables 1–4 illustrate that the analytical results really converge to FEM ones and that enough accuracy of the analytical solution can be achieved only considering the first four image points for this coated material. Figures 4 and 5 provide the numerical calculations based on the analytical solution ($n = 4$) for
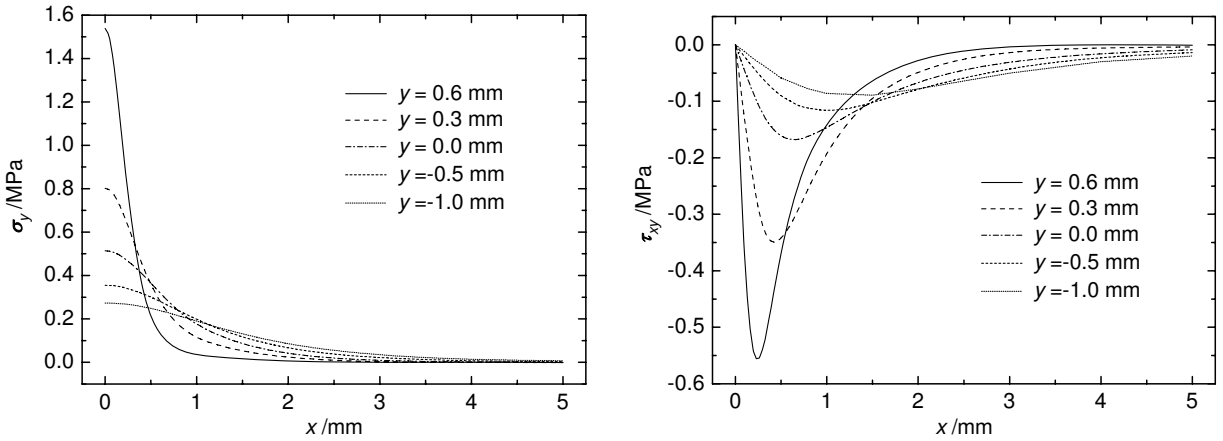
Figure 4. Analytical solutions of stress components at different values of y for the case of $F_x = 0$ and $F_y = 1\,\text{N}$: σ_y (left) and τ_{xy} (right).
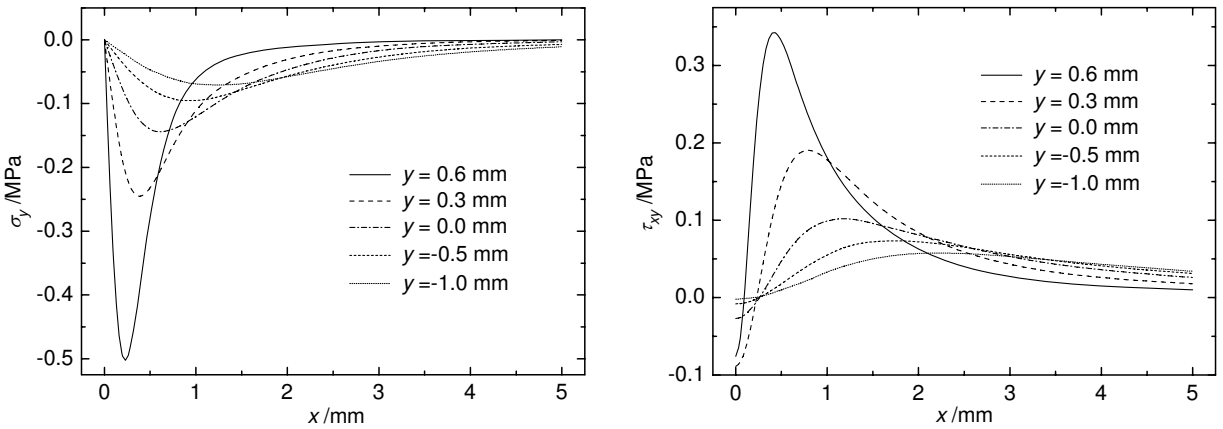

Figure 5. Analytical solutions of stress components at different values of y for the case of $F_x = 1\,\text{N}$ and $F_y = 0$: σ_y (left) and τ_{xy} (right).

the stress components at different locations for the cases of $F_x = 0$ and $F_y = 1\,\text{N}$ as well as $F_x = 1\,\text{N}$ and $F_y = 0$, respectively.

On the other hand, to maintain the accuracy of the analytical solution, the different orders of image points should be needed for the various matches of material constants. Given $\nu_{\text{I}} = \nu_{\text{II}} = 0.3$ and $E_{\text{I}} = 546\,\text{GPa}$, Figure 6 displays the required image point order to obtain the results with the relative error below 2.5%. It can be found that the larger the difference of the material constants is, the more image points are needed.

5. Conclusions

In this paper, we derived the analytical solution for the plane problem of the coated material subjected to an arbitrary concentrated force on the free surface by using the general solution of the displacement
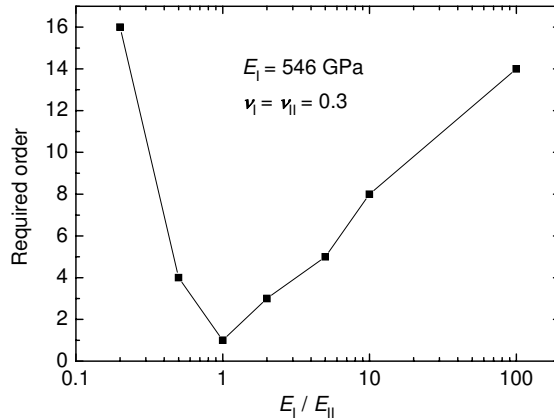
Figure 6. Image point order required for various Young's modulus ratios.

method as well as the image point method. This solution is given explicitly as the summation of the harmonic functions corresponding to each image point, and the harmonic functions corresponding to the higher-order image points can be determined from those to the lower-order ones through the recurrence. The numerical results verified the correctness and rapid convergence of the analytical solution obtained in this paper. The enough accurate theoretical results can be obtained only by considering image points of the first several order.

References

[Aderogba 2003] K. Aderogba, "An image treatment of elastostatic transmission from an interface layer", *J. Mech. Phys. Solids* **51**:2 (2003), 267–279.

[Barnett and Lothe 1974] D. Barnett and J. Lothe, "An image force theorem for dislocations in anisotropic bicrystals", *J. Phys. F Metal Phys.* **4**:10 (1974), 1618–1635.

[Djabella and Arnell 1993] H. Djabella and R. Arnell, "Finite element comparative study of elastic stresses in single, double layer and multilayered coated systems", *Thin Solid Films* **235**:1-2 (1993), 156–162.

[Dundurs and Hetényi 1965] J. Dundurs and M. Hetényi, "Transmission of force between two semi-infinite solids", *J. Appl. Mech.* (*ASME*) **32** (1965), 671–674.

[Hasegawa et al. 1992] H. Hasegawa, V.-G. Lee, and T. Mura, "Green's functions for axisymmetric problems of dissimilar elastic solids", *J. Appl. Mech.* (*ASME*) **59**:2 (1992), 312–320.

[Hiroyuki et al. 1994a] K. Hiroyuki, I. Masahiro, T. Tohru, and K. Hiroki, "Approximate expression for stress distribution in film subjected to indentation by spherical indenter : the case of a very thin film", *Trans. Soc. Mech. Eng. A* **60**:570 (1994), 416–420.

[Hiroyuki et al. 1994b] K. Hiroyuki, I. Masahiro, T. Tohru, and K. Hiroki, "Elasto-plastic finite-element analysis of stress distribution in a film-substrate system indented by a spherical indenter in relation to evaluation of fracture strength of films", *Trans. Soc. Mech. Eng. A* **60**:570 (1994), 409–415.

[Kouitat-Njiwa and von Stebut 2003] R. Kouitat-Njiwa and J. von Stebut, "Boundary element numerical analysis of elastic indentation of a sphere into a bi-layer material", *Int. J. Mech. Sci.* **45**:2 (2003), 317–324.

[Li and Xu 2007] Y. Li and J.-Q. Xu, "Fundamental solution for bonded materials with a free surface parallel to the interface. Part II: Solutions of concentrated force acting at the interior of the substrate and the case when the force acting at the interface", *Int. J. Solids Struct.* **44**:10 (2007), 3317–3327.

[Li et al. 2004] Y. Li, J.-Q. Xu, and L. Fu, "Fundamental solution for bonded materials with a free surface parallel to the interface. Part I: Solution of concentrated forces acting at the inside of the material with a free surface", *Int. J. Solids Struct.* **41**:24-25 (2004), 7075–7089.

[Ma and Lee 2009] C.-C. Ma and J.-M. Lee, "Theoretical analysis of generalized loadings and image forces in a planar magnetoelectroelastic layered half-plane", *J. Mech. Phys. Solids* **57**:3 (2009), 598–620.

[Ma and Lin 2001] C.-C. Ma and R.-L. Lin, "Image singularities of Green's functions for an isotropic elastic half-plane subjected to forces and dislocations", *Math. Mech. Solids* **6**:5 (2001), 503–524.

[Ma and Lin 2002a] C.-C. Ma and R.-L. Lin, "Full-field analysis of a planar anisotropic layered half-plane for concentrated forces and edge dislocations", *Proc. Royal Soc. London A Math. Phys. Eng. Sci.* **458**:2026 (2002), 2369–2392.

[Ma and Lin 2002b] C.-C. Ma and R.-L. Lin, "Image singularities of Green's functions for isotropic elastic bimaterials subjected to concentrated forces and dislocations", *Int. J. Solids Struct.* **39**:20 (2002), 5253–5277.

[Masayuki et al. 1994] T. Masayuki, I. Takeshi, K. Ken, and A. Masao, "Asymmetric three-point bending of a laminated beam containing a delamination", *Trans. Soc. Mech. Eng. A* **60**:578 (1994), 2266–2272.

[Mindlin 1936] R. Mindlin, "Force at a point in the interior of a semi-infinite solid", *J. Appl. Phys.* **7** (May 1936), 195–202.

[Mindlin and Cheng 1950] R. Mindlin and D. H. Cheng, "Nuclei of strain in the semi-infinite solid", *J. Appl. Phys.* **21** (September 1950), 926–930.

[Phan-Thien 1983] N. Phan-Thien, "On the image system for the Kelvin-state", *J. Elasticity* **13** (1983), 231–235.

[Rongved 1955] L. Rongved, "Force interior to one of two jointed semi-infinite solids", pp. 1–13 in *Proceedings of the 2nd Midwestern Conference on Solid Mechanics*, 1955.

[Takuma et al. 2000] M. Takuma, N. Shinke, T. Kubo, and A. Yonekura, "Evaluation on fracture characteristics of thin ceramic film with scratch testing", *Trans. Soc. Mech. Eng. A* **66**:651 (2000), 2074–2078.

[Ting 1992] T. C. T. Ting, "Image singularities of green's functions for anisotropic elastic half-spaces and bimaterials", *Quarterly J. Mech. Appl. Math.* **45**:1 (1992), 119–139.

[Willis 1970] J. Willis, "Stress fields produced by dislocations in anisotropic media", *Philos. Mag.* **21** (May 1970), 931–949.

[Wu and Liu 2008] Z. Wu and Y. Liu, "Analytical solution for the singular stress distribution due to V-notch in an orthotropic plate material", *Eng. Fract. Mech.* **75**:8 (2008), 2367–2384.

[Xu and Mutoh 2003a] J.-Q. Xu and Y. Mutoh, "Analytical solution for interface stresses due to concentrated surface force", *Int. J. Mech. Sci.* **45**:11 (2003), 1877–1892.

[Xu and Mutoh 2003b] J.-Q. Xu and Y. Mutoh, "A normal force on the free surface of a coated material", *J. Elasticity* **73** (2003), 147–164.

[Yang and Xu 2009] Z. Yang and J.-Q. Xu, "Three-dimensional solution of concentrated forces in semi-infinite coating materials", *Int. J. Mech. Sci.* **51**:6 (2009), 424–433.

ZHIGEN WU: zhigenwu@126.com
Hefei University of Technology, School of Civil Engineering, Hefei, 230009, China

YIHUA LIU: liuyhfut@yahoo.cn
Hefei University of Technology, School of Civil Engineering, Hefei, 230009, China

CHUNXIAO ZHAN: zhcxhfut@yahoo.cn
Hefei University of Technology, School of Civil Engineering, Hefei, 230009, China

MEIQIN WANG: wang_meiqin@yahoo.cn
Hefei University of Technology, School of Civil Engineering, Hefei, 230009, China

JOURNAL OF MECHANICS OF MATERIALS AND STRUCTURES

http://www.jomms.org

Founded by Charles R. Steele and Marie-Louise Steele

Journal of Mechanics of Materials and Structures

Volume 5, No. 6   June 2010